A Unified Dark Matter Model in sUED

Yang Bai[a] and **Zhenyu Han**[b]

[a]*Fermi National Accelerator Laboratory, P.O. Box 500, Batavia, IL 60510, USA*
[b]*Department of Physics, University of California, Davis, CA 95616, USA*

Abstract

We propose a dark matter model with standard model singlet extension of the universal extra dimension model (sUED) to explain the recent observations of ATIC, PPB-BETS, PAMELA and DAMA. Other than the standard model fields propagating in the bulk of a 5-dimensional space, one fermion field and one scalar field are introduced and both are standard model singlets. The zero mode of the new fermion is identified as the right-handed neutrino, while its first KK mode is the lightest KK-odd particle and the dark matter candidate. The cosmic ray spectra from ATIC and PPB-BETS determine the dark matter particle mass and hence the fifth dimension compactification scale to be 1.0–1.6 TeV. The zero mode of the singlet scalar field with a mass below 1 GeV provides an attractive force between dark matter particles, which allows a Sommerfeld enhancement to boost the annihilation cross section in the Galactic halo to explain the PAMELA data. The DAMA annual modulation results are explained by coupling the same scalar field to the electron via a higher-dimensional operator. We analyze the model parameter space that can satisfy the dark matter relic abundance and accommodate all the dark matter detection experiments. We also consider constraints from the diffuse extragalactic gamma-ray background, which can be satisfied if the dark matter particle and the first KK-mode of the scalar field have highly degenerate masses.

1 Introduction

Recently, there have been many pieces of evidence on detection of dark matter from either direct searches or indirect searches. The DAMA/LIBRA collaboration has published their new results and confirmed and reinforced their detection of an annual modulation in their signal rate. Combined with the DAMA/NaI data, they have interpreted this observation as evidence for dark matter particles at the 8.2σ confidence level [1]. The ATIC-2 experiment has reported an excess in its preliminary $e^+ + e^-$ data at energies of $500 - 800$ GeV [2]. This is confirmed recently by the PPB-BETS balloon experiment [3]. It can be naturally explained by dark matter annihilation intro electrons and positrons. The PAMELA collaboration has published their results and shown that an anomalous increase of the positron fraction in the energy range of $10 - 100$ GeV [4]. All of those experimental results indicate detection of dark matter in our universe. In this paper, we are trying to explain all those experiments in terms of a concrete particle physics model.

There are well motivated models containing unbroken discrete symmetries and providing dark matter candidates in the literature. In the extensively studied MSSM, the R-parity protects the neutralino from decaying [5]. In the Universal Extra Dimension model (UED) [6], the KK-parity keeps the lightest KK-odd particle stable and therefore also provides a dark matter candidate [7]. In this paper, we focus on the explanation of dark matter experiments based on the UED model. However, in the minimal UED model, the dark matter candidate, KK-photon, is difficult to account for the PAMELA results because of their small annihilation rate to electrons and positrons in the Galactic halo. Recent studies have shown that the PAMELA results can be explained if the dark matter particles mainly annihilate into a pair of electrons and there exists a large boost factor to increase the annihilation cross section in the Galactic halo [8]. The large boost factor can be obtained through the Sommerfeld enhancement effect if there is a new long-range force attractive between two dark matter particles [9] (see also [10] for other particle physics models that explain the PAMELA results). If the particle mediating the long-range force only couples to electrons, then the elastic scattering of dark matter to the electron may explain the DAMA results without contradicting the null results from other direct dark matter experiments like CDMS [11] and XENON [12].

Hence, additional ingredients are needed in the UED model. In this paper, we explore this possibility by studying the standard model singlet extension of the UED model (sUED). Other than the standard model (SM) fields propagating in the 5-dimensional bulk, we introduce two

new SM singlet fields: one fermion field and one scalar field. The zero mode of the fermion field ν_R plays the role of the right-handed neutrino and generates neutrino Majorana mass through the see-saw mechanism. The first KK-mode of the fermion field contains two Weyl fermions with the lightest one called χ_- as the lightest KK-odd particle. To simplify our discussions, we only include one generation of right-handed neutrinos, while it is easy to extend our model by including more generations of right-handed neutrinos. The zero mode of the scalar field s_0 is chosen to have a mass below 1 GeV, couples to the right-handed neutrino fields through a renormalizable operator and hence provides a long-range force for the dark matter candidate χ_-. In order to explain the PAMELA results, we also couple the light scalar field s_0 to the electron field through a higher-dimensional operator and let s_0 mainly decay into a pair of electrons. The same coupling of s_0 to the electron field can also generate a large elastic scattering cross section betweeen χ_- and the electron to explain the DAMA results.

The paper is organized as following. In section 2, we show specifically the particles and the Lagrangian of our model. We analyze the spectrum of our particles and identify χ_- as the lightest KK-odd particle and the dark matter candidate. While in section 3, we calculate the relic abundance of the dark matter candidate. We also take the co-annihilation effects into account in this section. We illustrate how to accommodate the ATIC-2, PPB-BETS and PAMELA results and DAMA results in section 4 and in section 5, respectively. In section 6, we show how to evade the diffuse extragalactic gamma-ray background today by making two KK-odd particle highly degenerate and suppressing the kinetic decoupling temperature of dark matter. Finally, we briefly summarize the conclusion of this paper in section 7.

2   The Model

We consider all SM fields, a new SM singlet fermion field N and a new SM singlet scalar field S, propagating in one extra dimension, which is compactified on an orbifold, S^1/Z_2 with the fundamental region $0 \leq y \leq \pi R$. We have the action of our model as following

$$
\begin{aligned}
S_{5D} &= \int d^4x \int_0^{\pi R} dy \left[\mathcal{L}_{SM} - \sqrt{\pi R}\, y_\nu \, \bar{L}\, \tilde{H}\, N - \frac{1}{2}\, m\, N^T \mathcal{C}_5\, N - \frac{1}{2}\, \mu^2\, S^2 \right. \\
&\left. - (\pi R)^2\, y_e'\, S\, \bar{L}\, H\, E - (\pi R)^2\, y_D'\, S\, \bar{L}\, \tilde{H}\, N - \frac{1}{2}\, \sqrt{\pi R}\, y_M\, S\, N^T \mathcal{C}_5\, N + h.c. \right]. \quad (1)
\end{aligned}
$$

Here, y_ν and y_i' are dimensionless parameters; L is a $SU(2)$ doublet and gives us the four-dimensional field $\ell_L = (\nu_L, e_L)^T$; N contains the right-handed neutrino ν_R as its zero mode;

$\mathcal{C}_5$ is the 5-d charge-conjugate operator, $\mathcal{C}_5 \equiv i\,\gamma_0\gamma_2\gamma_5$ [14]. In our analysis, we will neglect the family indices, but note that it is easy to extend our model to include more generations of fermions.

The scalar field, S, is decomposed into 4-d fields as

$$S(x^\mu, y) = \frac{1}{\sqrt{\pi R}} \left[s_0(x^\mu) + \sqrt{2} \sum_{j \geq 1} s_j(x^\mu) \cos\left(\frac{j\,y}{R}\right) \right]. \tag{2}$$

The 5-d spinor field $N \equiv (\xi, \bar{\eta})^T$, with $\bar{\eta} \equiv i\,\sigma_2\,\eta^*$. We choose the Neumann-Neumann boundary condition for the ξ and hence the Dirichlet-Dirichlet boundary condition for η. ν_R is the zero mode of ξ. The fields ξ and η are decomposed as

$$\xi(x^\mu, y) = \frac{1}{\sqrt{\pi R}} \left[\nu_R(x^\mu) + \sqrt{2} \sum_{j \geq 1} [\xi_j(x^\mu) \cos\left(\frac{j\,y}{R}\right)] \right], \tag{3}$$

$$\eta(x^\mu, y) = \sqrt{\frac{2}{\pi R}} \sum_{j \geq 1} [\eta_j(x^\mu) \sin\left(\frac{j\,y}{R}\right)]. \tag{4}$$

After integrating out the fifth dimension and the eletroweak symmetry breaking, we arrive at the following 4-d Lagrangian

$$
\begin{aligned}
-\mathcal{L}_{4d} = {}& y_\nu\, v\, \bar{\nu}_L\, \nu_R + \frac{1}{2}\, m\, \nu_R^T\, i\sigma_2\, \nu_R + \frac{1}{2}\, \mu^2\, s_0^2 + y_e\, s_0\, \bar{e}_L\, e_R + y_D\, s_0\, \bar{\nu}_L\, \nu_R + \frac{1}{2}\, y_M\, s_0\, \nu_R^T\, i\sigma_2\, \nu_R \\
& + \frac{1}{2}\, (\mu^2 + \frac{1}{R^2})\, s_1^2 + \frac{1}{2}\, m\, (\xi_1^T\, i\sigma_2\, \xi_1 + \eta_1^T\, i\sigma_2\, \eta_1) + \frac{1}{R}\, \eta_1^T\, i\sigma_2\, \xi_1 \\
& + y_D\, s_1\, \bar{\nu}_L\, \xi_1 + \frac{1}{2}\, y_M\, s_0\, (\xi_1^T\, i\sigma_2\, \xi_1 + \eta_1^T\, i\sigma_2\, \eta_1) + y_M\, s_1\, \xi_1^T\, i\sigma_2\, \nu_R + h.c. + \cdots. \tag{5}
\end{aligned}
$$

Here we only keep the zeroth and first KK modes of the particles in the Lagrangian; $v = 174\,\mathrm{GeV}$ is the vacuum expectation value of the Higgs boson; $y_e \equiv y'_e\, \pi\, v\, R$ and $y_D \equiv y'_D\, \pi\, v\, R$. In the mass eigenbasis, $\chi_- \equiv i\,(\xi_1 - \eta_1)/\sqrt{2}$ and $\chi_+ \equiv (\xi_1 + \eta_1)/\sqrt{2}$, we have

$$
\begin{aligned}
-\mathcal{L}_{4d} = {}& \frac{1}{2}\, m_\nu\, \nu_L^T\, i\sigma_2\, \nu_L + \frac{1}{2}\, m\, \nu_R^T\, i\sigma_2\, \nu_R + \frac{1}{2}\, \mu^2\, s_0^2 + y_e\, s_0\, \bar{e}_L\, e_R + y_D\, s_0\, \bar{\nu}_L\, \nu_R \\
& + \frac{1}{2}\, y_M\, s_0\, \nu_R^T\, i\sigma_2\, \nu_R + \frac{1}{2}\, M_s^2\, s_1^2 + \frac{1}{2}\, M_+\, \chi_+^T\, i\sigma_2\, \chi_+ + \frac{1}{2}\, M_-\, \chi_-^T\, i\sigma_2\, \chi_- \\
& + \frac{y_D}{\sqrt{2}}\, s_1\, \bar{\nu}_L\, \chi_+ - \frac{i\,y_D}{\sqrt{2}}\, s_1\, \bar{\nu}_L\, \chi_- + \frac{1}{2}\, y_M\, s_0\, (\chi_+^T\, i\sigma_2\, \chi_+ - \chi_-^T\, i\sigma_2\, \chi_-) \\
& + \frac{y_M}{\sqrt{2}}\, s_1\, \chi_+^T\, i\sigma_2\, \nu_R - \frac{i\,y_M}{\sqrt{2}}\, s_1\, \chi_-^T\, i\sigma_2\, \nu_R + h.c. + \cdots. \tag{6}
\end{aligned}
$$

3

Here $m_\nu = y_\nu^2 v^2/m$ is the left-handed neutrino mass through the see-saw mechanism (we will choose the energy scale for m to be around one GeV, so y_ν needs to be very small to fit the neutrino mass); the right-handed neutrino mass is approximately m assuming $y_\nu v \ll m$; $M_s^2 = (\mu^2 + 1/R^2)$, the mass of the first KK mode of the scalar field; $M_\pm = 1/R \pm m$ and are positive for $m \ll 1/R$; $2\,m_e < \mu < m$, so the right-handed neutrio v_R can decay to v_L plus s_0, and s_0 can decay to two electrons. In the minimal UED model, after taking radiative corrections into account, all first KK modes have masses above the compactification scale $1/R$ [25]. The fermion Yukawa coupling and the scalar quartic coupling in general will lower the first KK-mode masses. Therefore, we anticipate that after radiative corrections, the three new KK-odd particles s_1, χ_+ and χ_- have masses below other SM KK modes. Due to theoretic uncertainties including Brane-localized terms, we will keep their masses as free parameters. Furthermore, we assume $M_+ > M_s > M_-$, therefore the lightest KK-odd particle χ_- is the dark matter candidate in this model. The χ_+ field decays into s_1 plus ν_L, while s_1 mainly decays into χ_- plus ν_L when $M_s - M_- < m$ (the decay channel of s_1 to χ_- plus ν_R is kinematically forbidden).

3 Annihilation, Co-annihilation and Relic Abundance

The present relic abundance of dark matter is related to pair-annihilation rates in the non-relativistic limit by the sum of the quantities, $a(X) = \langle v\,\sigma \rangle$ with $v \sim 0.3$ to be the relative velocity between the dark matter particles. For simplicity, we only consider s-wave channel annihilation in this paper because the p-wave channel is suppressed by $\mathcal{O}(v^2)$. The present dark matter abundance from WMAP collaboration, $0.096 < \Omega\,h^2 < 0.122\,(2\sigma)$, requires $a_{\text{tot}} = 0.81 \pm 0.09\,\text{pb}$ [26][27], assuming the dark matter candidate in our model can make up all the dark matter.

Since the three lightest KK-odd particles has almost degenerate masses in our model, we need to consider co-annihilation among those particles. The effective annihilation cross section [15] is

$$\sigma_{\text{eff}} = \sum_{ij}^{3} \sigma_{ij} \frac{g_i g_j}{g_{\text{eff}}^2} (1 + \Delta_i)^{3/2} (1 + \Delta_j)^{3/2} e^{-x(\Delta_i + \Delta_j)} , \qquad (7)$$

with $\sigma_{ij} = \sigma(X_i X_j \to \text{SM particles})$. Here, X_i represents the three lightest particles in our model with $i = 1$ for χ_-, $i = 2$ for χ_+ and $i = 3$ for s_1; $\Delta_i = (M_i - M_-)/M_-$; g_i is the number of degrees of freedom of the i's particle and $g_{1,2} = 2$ for $\chi_\pm$ and $g_3 = 1$ for s_1; g_{eff} is defined to

be

$$g_{\text{eff}} = \sum_i^3 g_i \left(1 + \Delta_i\right)^{3/2} e^{-x\,\Delta_i}. \tag{8}$$

To simplify our calculation, we will choose $x = x_{\text{F}} = M_-/T_{\text{F}} \approx 20$ (T_F is the dark matter freeze-out temperature). The dark matter mass constrained from the relic abundance only slightly depends on the freeze-out temperature. When the three lightest KK-odd particles have nearly degenerate masses or satisfy $\Delta_i < 0.01$, which is the case in our model, we have

$$\sigma_{\text{eff}} = \frac{4}{25}(\sigma_{--} + 2\,\sigma_{-+} + \sigma_{++}) + \frac{4}{25}(\sigma_{-s} + \sigma_{+s}) + \frac{1}{25}\sigma_{ss}. \tag{9}$$

For $y_e\,, y_D \ll y_M$, which is the parameter region of our interests, we only keep the largest Yukawa coupling y_M in calculating the annihilation cross section. The dominant self-annihilation channel of χ_-'s is $\chi_- \chi_- \to \nu_R \nu_R$ in the t-channel by exchanging the s_1 field (the s-channel diagram by exchanging s_0 field has zero contributions to the s-wave annihilation, and is neglected here. For the same reason, we also neglect the annihilation channel $\chi_- \chi_- \to s_0 s_0$). To leading order in the relative velocity, v, of two χ_-'s and neglecting ν_R mass in the limit $m \ll 1/R$, the annihilation cross section is

$$v\,\sigma_{--} = \frac{y_M^4\, M_-^2}{64\,\pi\,(M_-^2 + M_s^2)^2} + \mathcal{O}(v^2). \tag{10}$$

The annihilation cross section σ_{++} of $\chi_+ \chi_+ \to \nu_R \nu_R$ has a similar formula by replacing M_- with M_+. The co-annihilation cross section of $\chi_- \chi_+ \to \nu_R \nu_R$ is from the t-channel diagram by exchanging s_1 and has the formula

$$v\,\sigma_{-+} = \frac{y_M^4\,(M_- + M_+)^2}{256\,\pi\,(M_-\,M_+ + M_s^2)^2} + \mathcal{O}(v^2). \tag{11}$$

The co-annihilation cross section σ_{-s} of $\chi_- s_1 \to s_0 \nu_R$ by exchanging χ_- in the t-channel is calculated to be

$$v\,\sigma_{-s} = \frac{y_M^4\,(M_- - M_s)^2}{64\,\pi\,M_-^2\,M_s\,(M_- + M_s)} + \mathcal{O}(v^2). \tag{12}$$

A similar formula for σ_{+s} can be obtained by changing M_- to M_+. Finally, for the self-annihilation of s_1, the annihilation process is $s_1 s_1 \to \nu_R \nu_R$ by exchanging χ_- and χ_+ in the t-channel. It has the following formula

$$v\,\sigma_{ss} = \frac{y_M^4\,(M_- - M_+)^2\,(M_s^2 - M_1 M_2)^2}{8\,\pi\,(M_s^2 + M_-^2)^2\,(M_s^2 + M_+^2)^2} + \mathcal{O}(v^2). \tag{13}$$

5

When M_-, M_+ and M_s are nearly degenerate, we use the parameter M_- to represent those three variables. From Eq. (9), we have

$$v\,\sigma_{\text{eff}} \;=\; \frac{y_M^4}{400\,\pi\,M_-^2} \;+\; \mathcal{O}(v^2)\,. \tag{14}$$

Therefore, the quantity a_{tot} in our model is

$$a_{\text{tot}} \;=\; \frac{y_M^4}{400\,\pi\,M_-^2} \;\approx\; y_M^4\,(\frac{1\,\text{TeV}}{M_-})^2 \times 0.32\,\text{pb}\,. \tag{15}$$

For the dark matter mass of $1-1.6$ TeV, we need to choose $y_M \approx 1.2-1.6$ to satisfy the current dark matter relic abundance.

4   ATIC, PPB-BETS and PAMELA

The ATIC-2 balloon experiment reported an excess in the $e^+ + e^-$ energy spectrum between $500 - 800$ GeV [2]. This is confirmed recently by the PPB-BETS balloon experiment [3]. One explanation of this excess is that the dark matter particles annihilate into electrons.

Specific to our model, the dark matter candidate χ_- mainly annihilates to right-handed neutrinos ν_R, which subsequently decays into $\nu_L + s_0$. Because the s_0 has a mass below ν_R and above twice of the electron mass, it dominantly decays into two electrons. The chain of this process is

$$\chi_-\,\chi_- \;\rightarrow\; \nu_R\,\nu_R \;\rightarrow\; \nu_L\,s_0\,\nu_L\,s_0 \;\rightarrow\; \nu_L\,e^+\,e^-\,\nu_L\,e^+\,e^-\,. \tag{16}$$

and the Feynman diagram is shown in Fig. 1

Neglecting all particles' masses except χ_- and s_1, each of the four electrons has a nearly flat energy spectrum with the maximum energy of a half of the dark matter mass M_-. This
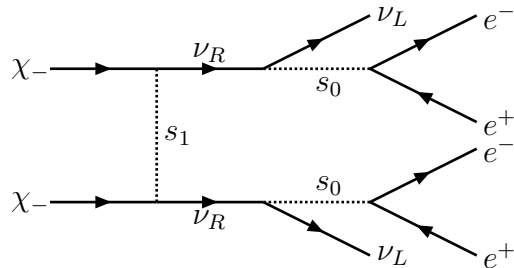

Figure 1: Feynman diagram of the main annihilation channel of χ_- in our model.

is because each right-handed neutrino ν_R carries energy of the dark matter mass M_-. After it decays into a fermion and a scalar, the scalar field s_0 carries approximately a half of ν_R energy. Because two fermions e^+ and e^- has an isotropic distribution in the s_0 rest-frame, each electron has an flat energy spectrum with the maximum energy to be a half of the dark matter mass. Numerically, we show the energy density distribution in Fig. 2, which is calculated using Calchep [16]. As can be seen from Fig. 2, the positron energy density distribution has a flat
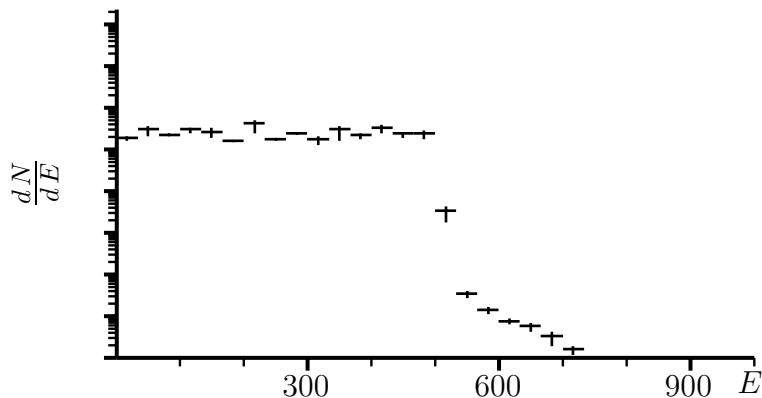
Figure 2: The energy density distribution as a function of the positron energy for 1 TeV dark matter mass. The errors on this plot come from uncertainties of numerical simulations.

spectrum with the upper limit to be a half of the dark matter mass. Since the products of the annihilation contains mainly leptons, we should anticipate the observation of an excess in positrons and not in anti-protons [17]. In order to explain the ATIC-2 results, the dark matter mass M_- in our model should be from 1 TeV to 1.6 TeV. Hence, from Eq. (14) the Yukawa coupling y_M needs to be from 1.2 to 1.6 to provide the right relic abundance of dark matter.

The PAMELA data [4] show a steep increase in the energy spectrum of the positron fraction $e^+/(e^+ + e^-)$ in cosmic rays above 10 GeV. Several groups have analyzed the dark matter explanation of this observation and found that for two to two annihilation of dark matter to two electrons a large boost factors are needed to fit the PAMELA data [8]. Depending on diffusion parameters, a boost factor of a few hundred is required in general. In our model, we have four electrons in the final state. The maximal energy for each electron is a half of the dark matter mass and is between 500 GeV to 800 GeV. Taking radiation into account, we anticipate a continuous spectrum with an edge close to $M_-/2$. To explain the PAMELA data, a boost factor from Sommerfeld enhancement is needed to fit the observed positron spectrum. In our model,

the light visible particle s_0 provides a long range force between the dark matter candidate χ_- and induces a Yukawa potential between two χ_-'s. Neglecting the contact interaction, in the limit $\mu \ll y_M^2/(4\pi) M_-$, we use the Coulomb potential to calculate the boost factor due to Sommerfeld enhancement [9]

$$B \approx \frac{y_M^2}{4\, v_{\text{halo}}} \approx 360 \sim 640\,, \tag{17}$$

where $v_{\text{halo}} \approx 10^{-3}$ is the typical dark matter velocity in our Galaxy and $y_M = 1.2 \sim 1.6$ from the relic abundance calculation. From the analysis in [18], a boost factor around 300 for a flat electron energy spectrum with 800 GeV maximum energy provides a good fit to the PAMELA data. Therefore, up to astrophysical models or diffusion parameters, our model can accommodate the PAMELA data and at the same time satisfy the relic abundance.

5   DAMA

The DAMA collaboration reported an annual modulation in their DAMA/NaI experiment which have been recently confirmed by the DAMA/LIBRA experiment by the same collaboration. To reconcile the negative results from other direct searches such as CDMS, XENON-10 and CRESST-I, the authors of Ref. [13] proposed a scenario in which the dark matter particle interacts dominantly with the electron in the ordinary matter. In this case, bounds from other experiments can be avoided. For example, CDMS combines ionization, phonon and timing information to reject events from electron recoils. Similarly, XENON rejects electron recoils based on the ionization/scintillation ratio. In contrast, the DAMA experiments are based on scintillation only, which can detect electron recoils with a low threshold. To release energy in the region where the annual modulation is observed (2-6 keV), elastic scatterings occur between the dark matter particles and the bound electrons with high momenta ($\sim O(1\,\text{MeV})$). In NaI (Tl), the bound electrons have a small but non-zero probability to have such high momenta.

   In our model, the DM-electron scattering is naturally realized by exchanging the scalar field s_0, which is also the mediator to generate the large boost factor to explain PAMELA. The corresponding Feynman diagram is shown in Fig. 3. In Ref. [13], the DAMA/NaI annual modulation data is analyzed to give a bound

$$1.1 \times 10^{-3}\,\text{pb/GeV} < \frac{\xi\, \sigma_e^0}{M_-} < 42.7 \times 10^{-3}\,\text{pb/GeV} \tag{18}$$

at 4σ from the null hypothesis, where ξ is the dark matter fraction of χ^- in the halo. In our case $\xi = 1$. The cross-section for DM-electron scattering at rest is denoted σ_e^0, and in our model
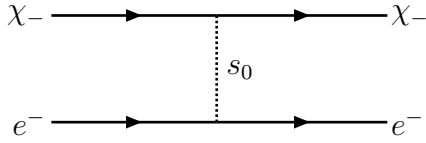
8

Figure 3: Feynman diagram of the DM-electron elastic scattering.

given by

$$\sigma_e^0 = \frac{y_e^2 \, y_M^2 \, m_e^2}{\pi \, \mu^4}.$$

(19)

The coupling y_e is also constrained by the electron $g-2$: $y_e \lesssim 2 \times 10^{-5} \, \mu/\text{MeV}$ (see Appendix A). Assuming $y_M = 1.2$ and $M_- = 1\,\text{TeV}$, we obtain the allowed region for μ and y_e from Eq. (18), as shown in Fig. 4. From Fig. 4, we see that μ is constrained to be $\lesssim O(100\,\text{MeV})$ and the corresponding y_e is consistent with the fact that it comes from a higher-dimensinal operator. Since that the results from the DAMA/LIBRA experiment confirm the DAMA/NaI results, we expect a significant allowed region still exists after including the DAMA/LIBRA data.
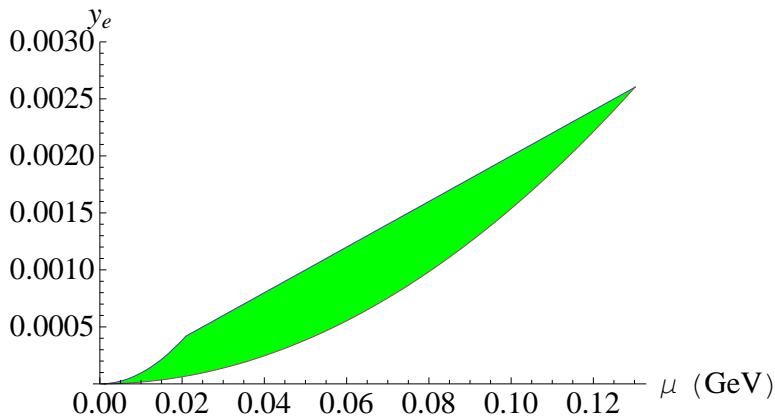

Figure 4: The allowed region (shaded) for μ vs y_e.

6   Early Annihilation and Diffuse Background

After dark matter falls out of chemical equilibrium, it may continue to interact with the standard model fields through elastic scattering. Therefore, the kinetic equilibrium temperature is in

9

general below the chemical freeze out temperature. The existing studies show that the kinetic decoupling temperature T_{kd} has a wide range from several MeV to a few GeV in the SUSY and MUED models [19]. This range of kinetic decoupling temperature implies a range of the smallest protohalos with a mass from $10^{-6} M_\oplus$ to $10^2 M_\oplus$.

Specific to our model, if the first scalar KK mode s_1 has a mass nearly degenerate with the mass of the dark matter field χ_-, there is an s-channel resonance enhancement for the elastic scattering cross section of χ_- with ν_L. Therefore, we see that a much lower kinetic decoupling temperature T_{kd} can happen in this model. The relevant Feynman diagram is shown in Fig. 5. When the neutrino energy E_ν is much less than the dark matter mass, the cross section of this elastic scattering process has the form

$$\sigma_\nu \;=\; \frac{y_D^4\, E_\nu^2}{16\,\pi\,[(M_-^2 - M_s^2)^2 + M_s^2\,\Gamma_s^2]} \;\approx\; \frac{y_D^4\, E_\nu^2}{16\,\pi\,(M_-^2 - M_s^2)^2}\,. \tag{20}$$

For the case $M_+ > M_s > M_-$ and $M_s - M_- < m$, s_1 decays into χ_- plus ν_L and the width of s_1 field is

$$\Gamma_s \;=\; \frac{y_D^2\,(M_s^2 - M_-^2)^2}{16\,\pi\,M_s^3}\,. \tag{21}$$

For $y_D < 1$, we neglect the width part in the propagator of s_1 and have the cross section only depending on the mass difference of s_1 and χ_-.

As the universe expands, the dark matter density and the elastic scattering rate, $\Gamma_\nu \equiv \langle v\,\sigma_\nu\rangle n_\nu$, decreases. Here n_ν is the number density of neutrinos, which are assumed to be in local thermal equilibrium and $v \approx 1$ in this case. Following the discussion in [20], the thermal average of σ_ν is

$$\langle \sigma_\nu\, v\rangle \;=\; \frac{9\,y_D^4\,T^2}{64\,\pi\,(M_-^2 - M_s^2)^2}\,. \tag{22}$$

As functions of temperature, $n_\nu \sim T^3$ and the Hubble rate of expansion $H \sim T^2/m_{\mathrm{pl}}$. The relaxation time τ defined as the time χ_-'s need to return to local thermal equilibrium after a deviation from it, and has a relation to the elastic scattering rate as $\tau(T) \approx \sqrt{2/3}\, M_-/(T\,\Gamma_\nu)$.
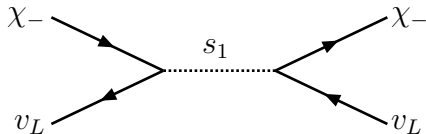
Figure 5: Feynman diagram of the elastic scattering of χ_- with ν_L.

The kinetic decoupling temperature of the dark matter candidate χ_- happens at $\tau(T_{\rm kd}) = 1/H(T_{\rm kd})$. The result is calculated as

$$T_{\rm kd} \approx \frac{2}{y_D} \left(\frac{M_-}{m_{\rm pl}} \right)^{1/4} \Delta \,, \tag{23}$$

where $\Delta^2 \equiv M_-^2 - M_s^2$. For example, when $M_- = 1.0$ TeV and $y_D = 0.1$, $T_{\rm kd}$ varies from 2 keV to 20 MeV for Δ between 1 MeV and 10 GeV. Using the relation between the mass of the first gravitational-bound structures and the kinetic decoupling temperature from [21]:

$$M_c \simeq 33 \left(T_{\rm kd}/10 \text{ MeV} \right)^{-3} M_\oplus \,, \tag{24}$$

we have the range of M_c to be $300 \, M_\oplus < M_c < 3 \times 10^{14} \, M_\oplus$ for Δ between 1 MeV and 10 GeV.

The χ_-'s in the dark-matter halos annihilate into electron-positron pairs in the energy of a few hundred GeV. The electrons and positrons rapidly inverse-Compton scatter with CMB photons and contribute to the diffuse extragalactic gamma-ray background today. The energy density in photons today from dark matter annihilation in the first halos is calculated in [22] and is

$$\rho_\gamma \approx 3 \times 10^{-9} \left(\frac{M_c}{10^{-6} \, M_\oplus} \right)^{-1/3} \text{ GeV cm}^{-3} \,. \tag{25}$$

The EGRET experiment imposes a bound on the extragalactic gamma-ray background [23]. It can be translated as $\rho_\gamma \leq 5.6 \times 10^{-17}(E_\gamma/\text{GeV})^{-1.11} \text{ GeV cm}^{-3}$. Therefore, this imposes a bound on the Δ, which indicates the mass difference of χ_- and s_1, as

$$\Delta \leq 3 \times 10^{-8} \, y_D \left(\frac{m_{\rm pl}}{M_-} \right)^{1/4} \left(\frac{E_\gamma}{\text{GeV}} \right)^{-1.11} \text{GeV} = \frac{y_D}{0.5} \left(\frac{M_-}{2 \text{ TeV}} \right)^{-1/4} \left(\frac{E_\gamma}{\text{GeV}} \right)^{-1.11} 0.1 \text{ MeV} \,. \tag{26}$$

The access energy range of E_γ in EGRET is from 30 MeV to 100 GeV. This means that a highly degenerate spectrum between χ_- and s_1 up to order of keV is needed to evade the current bound on the diffuse background.

7   Discussions and Conclusions

At the LHC, the production mechanism of the KK-odd particles in our model is similar to the minimal UED model. Unlike the minimal UED model, the KK mode of the right-handed neutrino χ_- is the lightest KK-odd particle. Hence all other first KK-odd modes of SM particles should subsequently decay into χ_-. Interestingly, the KK photon B^1, which is the lightest

KK-odd particle in the minimal UED, decays into s_1 plus two electrons through an off-shell intermediate KK electron exchanging. The s_1 subsequently decays into χ_- and ν_L. If the mass difference between B^1 and χ_- is a few 10 GeV, there will be lots of energetic leptons generated at the LHC [28]. After accommodating the DAMA results and being consistent with the electron $g - 2$, the relevant coupling y_e, which also determines the width of B^1, is of order 10^{-3}. Hence the width of B^1 is estimated to be $\sim y_e^2 \, e^2 \, \Delta M/(64 \, \pi^3)$ with the $\Delta M^2 = M_{B^1}^2 - M_-^2$ and is of order eV.

Since the products of the dark matter annihilation contain electrons and positrons as well as neutrinos, the Super-Kamiokande may observe those energetic neutrinos from the sun [29]. When dark matter meets the sun, its speed will be slowed down due to its elastic scattering with electrons in the sun. Once the dark matter speed is reduced to be below the gravitational escaping velocity, it will be captured by the sun and produce additional neutrinos through annihilation. We leave this neutrinos flux calculation related to Super-Kamiokande to future study.

In conclusion, we have explored the sUED model, which is an extension of the UED model by including SM singlets, to explain the overwhelming evidence of the direct and indirect dark matter detections from experiments including DAMA, ATIC-2, PPB-BETS and PAMELA. The dark matter candidate is the first KK-mode of the right-haned neutrino χ_-, which is stable and protected by the KK-parity in the UED model from decaying.

The dark matter candidate χ_- mainly annihilates into the right-handed neutrino, which subsequently decays into the left-handed neutrino and s_0. The light scalar field s_0 below 1 GeV mainly decays into two electrons. Therefore, the final state particles of dark matter annihilation contain four electrons and two neutrinos. To explain the electron and positron energy spectrum observed by ATIC-2 and PPB-BETS, we found that the mass of the dark matter candidate should be from 1 TeV to 1.6 TeV, and hence sets the fifth dimension compactification scale. The PAMELA result is explained through the Sommerfeld enhancement effect due the long-range force between two dark matter particles by exchanging the light SM singlet scalar field s_0. The dark matter relic abundance determines the value of the Yukawa coupling of the dark matter to the scalar singlets. The same Yukawa coupling determines the boost factor from the Sommerfeld effect to be $360 - 640$ and suitable to explain the PAMELA resuts.

The DAMA results are explained by the elastic scattering of χ_- with electrons through exchanging the light scalar field s_0 in the t-channel. Since s_0 only couples to leptons, the null results of the dark matter direct searches at CDMS and XENON, which veto electron

recoils, are automatically explained. We have found that there exists parameter space in our model to accommodate the DAMA results without contradicting the electron $g - 2$. Finally, by calculating the s-channel elastic scattering cross section of χ_- with the left-handed neutrino by exchanging the first KK mode of the scalar field s_1, we show that the diffuse extragalactic gamma-ray background constrains can be satisfied provided that the masses of χ_- and s_1 are highly degenerate.

A   The constraint to y_e from electron $g - 2$.

The current experimental value for electron $g - 2$ is given by [30]

$$a_e = (1\,159\,652\,180.85 \pm .76) \times 10^{-12}\,. \tag{27}$$

Given uncertainties in the determination of α, extra contributions to a_e should satisfy [31]

$$|\delta a_e| \lesssim 2 \times 10^{-11}\,. \tag{28}$$

From the triangle diagram of s_0 exchange, we have [32]

$$\delta a_e = \frac{y_e^2}{8\,\pi^2}\,\widetilde{L}\,, \tag{29}$$

where

$$\widetilde{L} = \int_0^1 \mathrm{d}x\, \frac{x^2(2 - x)}{x^2 + (1 - x)(\mu/m_e)^2}\,. \tag{30}$$

When $\mu \gg m_e$, Eqs. (28), (29) and (30) give us

$$y_e \lesssim 2 \times 10^{-5} \frac{\mu}{\mathrm{MeV}}\,. \tag{31}$$

References

[1] R. Bernabei *et al.* [DAMA Collaboration], Eur. Phys. J. C **56**, 333 (2008) [arXiv:0804.2741 [astro-ph]].

[2] J. Chang et al. [ATIC Collaboration], *Prepared for 29th International Cosmic Ray Conference (ICRC 2005), 3, 1-4, Pune, India, Aug 03-10 2005*

[3] S. Torii *et al.*, arXiv:0809.0760 [astro-ph].

[4] O. Adriani *et al.*, arXiv:0810.4995 [astro-ph].

[5] G. Jungman, M. Kamionkowski and K. Griest, Phys. Rept. **267**, 195 (1996) [arXiv:hep-ph/9506380].

[6] T. Appelquist, H. C. Cheng and B. A. Dobrescu, Phys. Rev. D **64**, 035002 (2001) [arXiv:hep-ph/0012100].

[7] G. Servant and T. M. P. Tait, Nucl. Phys. B **650**, 391 (2003) [arXiv:hep-ph/0206071]; H. C. Cheng, J. L. Feng and K. T. Matchev, Phys. Rev. Lett. **89**, 211301 (2002) [arXiv:hep-ph/0207125]; D. Hooper and S. Profumo, Phys. Rept. **453**, 29 (2007) [arXiv:hep-ph/0701197].

[8] M. Cirelli and A. Strumia, arXiv:0808.3867 [astro-ph]; V. Barger, W. Y. Keung, D. Marfatia and G. Shaughnessy, arXiv:0809.0162 [hep-ph]; I. Cholis, L. Goodenough, D. Hooper, M. Simet and N. Weiner, arXiv:0809.1683 [hep-ph]; M. Cirelli, M. Kadastik, M. Raidal and A. Strumia, arXiv:0809.2409 [hep-ph].

[9] N. Arkani-Hamed, D. P. Finkbeiner, T. Slatyer and N. Weiner, arXiv:0810.0713 [hep-ph]; M. Pospelov and A. Ritz, arXiv:0810.1502 [hep-ph].

[10] J. H. Huh, J. E. Kim and B. Kyae, arXiv:0809.2601 [hep-ph]; C. R. Chen and F. Takahashi, arXiv:0810.4110 [hep-ph]; M. Fairbairn and J. Zupan, arXiv:0810.4147 [hep-ph]; A. E. Nelson and C. Spitzer, arXiv:0810.5167 [hep-ph]; Y. Nomura and J. Thaler, arXiv:0810.5397 [hep-ph]; R. Harnik and G. D. Kribs, arXiv:0810.5557 [hep-ph]; D. Feldman, Z. Liu and P. Nath, arXiv:0810.5762 [hep-ph]; Patrick Fox and Erich Poppitz, to appear.

[11] Z. Ahmed *et al.* [CDMS Collaboration], arXiv:0802.3530 [astro-ph].

[12] J. Angle *et al.* [XENON Collaboration], Phys. Rev. Lett. **100**, 021303 (2008) [arXiv:0706.0039 [astro-ph]].

[13] R. Bernabei *et al.*, Phys. Rev. D **77**, 023506 (2008) [arXiv:0712.0562 [astro-ph]].

[14] A. Pilaftsis, Phys. Rev. D **60**, 105023 (1999) [arXiv:hep-ph/9906265].

[15] K. Griest and D. Seckel, Phys. Rev. D **43**, 3191 (1991).

[16] A. Pukhov, arXiv:hep-ph/0412191.

[17] O. Adriani *et al.*, arXiv:0810.4994 [astro-ph].

[18] I. Cholis, D. P. Finkbeiner, L. Goodenough and N. Weiner, arXiv:0810.5344 [astro-ph].

[19] C. Boehm, P. Fayet and R. Schaeffer, Phys. Lett. B **518**, 8 (2001) [arXiv:astro-ph/0012504]; X. l. Chen, M. Kamionkowski and X. m. Zhang, Phys. Rev. D **64**, 021302 (2001) [arXiv:astro-ph/0103452]; S. Hofmann, D. J. Schwarz and H. Stoecker, Phys. Rev. D **64**, 083507 (2001) [arXiv:astro-ph/0104173]; S. Profumo, K. Sigurdson and M. Kamionkowski, Phys. Rev. Lett. **97**, 031301 (2006) [arXiv:astro-ph/0603373].

[20] S. Hofmann, D. J. Schwarz and H. Stoecker, Phys. Rev. D **64**, 083507 (2001) [arXiv:astro-ph/0104173]; A. M. Green, S. Hofmann and D. J. Schwarz, JCAP **0508**, 003 (2005) [arXiv:astro-ph/0503387].

[21] A. Loeb and M. Zaldarriaga, Phys. Rev. D **71**, 103520 (2005) [arXiv:astro-ph/0504112]; E. Bertschinger, Phys. Rev. D **74**, 063509 (2006) [arXiv:astro-ph/0607319].

[22] M. Kamionkowski and S. Profumo, arXiv:0810.3233 [astro-ph].

[23] P. Sreekumar *et al.* [EGRET Collaboration], Astrophys. J. **494**, 523 (1998) [arXiv:astro-ph/9709257].

[24] X. L. Chen and M. Kamionkowski, Phys. Rev. D **70**, 043502 (2004) [arXiv:astro-ph/0310473].

[25] H. C. Cheng, K. T. Matchev and M. Schmaltz, Phys. Rev. D **66**, 036005 (2002) [arXiv:hep-ph/0204342].

[26] A. Birkedal, K. Matchev and M. Perelstein, Phys. Rev. D **70**, 077701 (2004) [arXiv:hep-ph/0403004].

[27] Y. Bai, Phys. Lett. B **666**, 332 (2008) [arXiv:0801.1662 [hep-ph]].

[28] N. Arkani-Hamed and N. Weiner, arXiv:0810.0714 [hep-ph];

[29] S. Desai *et al.* [Super-Kamiokande Collaboration], Phys. Rev. D **70**, 083523 (2004) [Erratum-ibid. D **70**, 109901 (2004)] [arXiv:hep-ex/0404025].

[30] B. C. Odom, D. Hanneke, B. D'Urso and G. Gabrielse, Phys. Rev. Lett. **97**, 030801 (2006) [Erratum-ibid. **99**, 039902 (2007)]; G. Gabrielse, D. Hanneke, T. Kinoshita, M. Nio and B. C. Odom, Phys. Rev. Lett. **97**, 030802 (2006) [Erratum-ibid. **99**, 039902 (2007)].

[31] P. Fayet, Phys. Rev. D **75**, 115017 (2007) [arXiv:hep-ph/0702176].

[32] M. Krawczyk and J. Zochowski, Phys. Rev. D **55**, 6968 (1997) [arXiv:hep-ph/9608321].